Tectonophysics 592 (2013) 141–149

Contents lists available at SciVerse ScienceDirect

Tectonophysics

journal homepage: www.elsevier.com/locate/tecto

Precursory change in seismicity revealed by the Epidemic-Type Aftershock-Sequences model: A case study of the 1999 Chi-Chi, Taiwan earthquake

Masashi Kawamura *, Chien-chih Chen

Department of Earth Sciences and Graduate Institute of Geophysics, National Central University, Jhongli, Taoyuan 32001, Taiwan

ARTICLE INFO

Article history:
Received 6 September 2011
Received in revised form 19 December 2012
Accepted 7 February 2013
Available online 20 February 2013

Keywords:
ETAS model
Seismic precursor
Seismic quiescence
Seismic activation
The Chi-Chi earthquake

ABSTRACT

For gaining insight into the preparatory process of the 1999 Chi-Chi, Taiwan earthquake and its related statistical feature, the Epidemic-Type Aftershock-Sequences model (ETAS model) was applied to the earthquake data in Taiwan region. By means of the ETAS analysis for Taiwanese earthquakes larger than a magnitude of 2.4, we found seismic quiescence over broader regions of Taiwan. It was also found that inland areas near the epicenter of the Chi-Chi earthquake showed seismic activation in the period from Jan. 1, 1998 to Sep. 20, 1999, which is just before the occurrence of the Chi-Chi earthquake. The assumption that this is due to precursory slip (stress drop) on the fault plane of the Chi-Chi earthquake is supported by previous researches such as a numerical simulation using rate- and state-dependent friction laws and the observation of abnormal change in crustal displacement for a station of Taiwan GPS network near southern edge of the source area of the Chi-Chi earthquake.

1. Introduction

There are many reports on the existence of anomalous seismic activities, e.g. seismic activation and quiescence, prior to the occurrences of large earthquakes in seismically active regions around the world (Borovik et al., 1971; Bowman and King, 2001; Bowman et al., 1998; Bufe and Varnes, 1993; Bufe et al., 1994; Chen, 2003; Jaume and Sykes, 1999; Karakaisis et al., 2002; Mogi, 1969; Papazachos et al., 2010; Resenberg and Matthews, 1988; Sornette and Sammis, 1995; Sykes and Jaume, 1990; Wei et al., 1978; Wyss and Wiemer, 1997). These previous studies aim at the understanding of statistical feature and physical mechanism of the precursory seismic activity before a large earthquake. There is however no consensus on the underlying mechanism of precursory seismic activity though. Mignan (2011) summarized past various views of the statistical feature and occurrence mechanism of precursory seismic activity.

Taiwan is a representative region with high seismic activity that has historically been struck by large earthquakes. One example is the 1999 Chi-Chi earthquake (Mw 7.6), which occurred near the Chelungpu fault in the western part of central Taiwan on Sep. 21, 1999 and caused many casualties and traffic disruptions. Statistical features of seismic activity after the Chi-Chi earthquake, those of other physical processes triggered by the earthquake, and the precursory change in seismic activity have retrospectively been investigated by many researchers (Chen, 2003; Chen et al., 2005, 2010, 2011; Wu and Chen, 2007; Wu and Chiao, 2006; Wu et al., 2008). In particular as regards precursory change in seismic activity, Chen (2003) found seismic activation of moderate-sized earthquakes prior to the Chi-Chi event by examining the temporal change in the Gutenberg–Richter scaling distribution; Chen et al. (2005) indicated that there was anomalous seismic activity in the source area of the Chi-Chi earthquake prior to its occurrence by using the pattern informatics (PI) method (Chen et al., 2005, 2006; Holliday et al., 2005, 2006; Rundle et al., 2003; Tiampo et al., 2002a, 2002b; Wu et al., 2008); Wu and Chiao (2006) also found that, before the Chi-Chi event, a broader region around the source area of the Chi-Chi earthquake had revealed seismic quiescence using the *Z* test (Console et al., 2000; Habermann, 1988; Habermann and Wyss, 1984; Wiemer and Wyss, 1994); Wu and Chen (2007) then indicated seismic quiescence over a broad region of Eastern Taiwan and seismic activation near the epicenter of the Chi-Chi earthquake by the same *Z* test but using a longer earthquake catalog including both before and after the Chi-Chi event.

These reports imply that there was anomalous seismicity change associated with the Chi-Chi earthquake near its epicenter and over a broader region of Taiwan. For furthermore gaining insight into the preparatory process of the Chi-Chi earthquake, it is important to investigate the precursory change in seismic activity based on different approaches. With the motivation, we systematically applied the Epidemic-Type Aftershock-Sequences (ETAS) model (Ogata, 1988, 1992, 1999) to the earthquake data of Taiwan region. In the result, seismic quiescence over broader regions of Taiwan was confirmed. It was also found that inland areas near the epicenter of the Chi-Chi earthquake showed seismic activation in the period from Jan. 1, 1998 to Sep. 20, 1999 right before the Chi-Chi event. The spatial pattern of temporal changes in

* Corresponding author. Tel.: +886 3 422 7151x65663; fax: +886 3 422 2044.
E-mail address: mkawamu@ncu.edu.tw (M. Kawamura).

0040-1951/$ – see front matter © 2013 Elsevier B.V. All rights reserved.
http://dx.doi.org/10.1016/j.tecto.2013.02.017

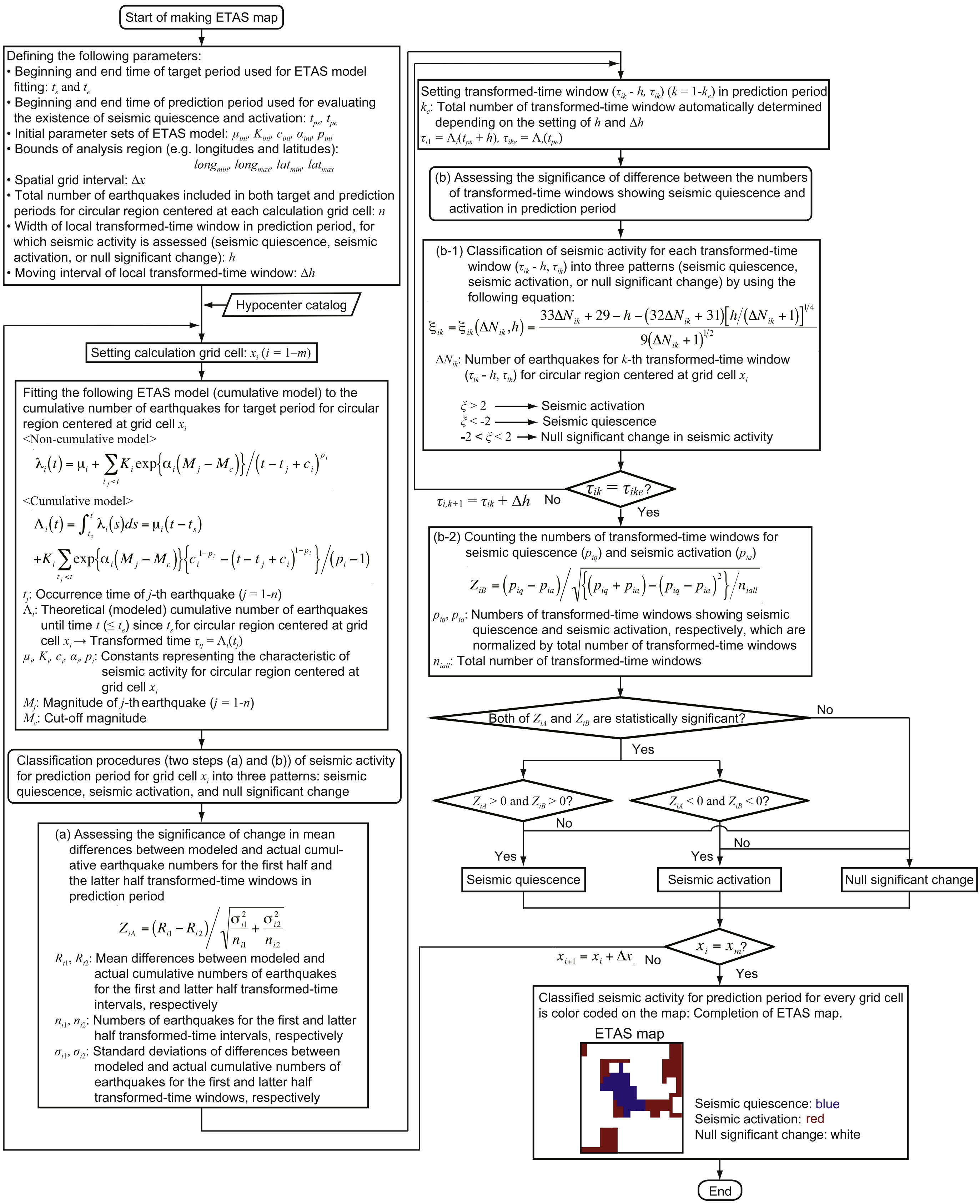

Fig. 1. Flowchart of ETAS analysis procedure for classifying seismic activity in prediction period for each grid cell into three patterns: seismic quiescence, seismic activation, and null significant change.

seismic activities obtained by the ETAS analysis turned out to be robust because the areas of seismic activation and quiescence were obtained by the ETAS analysis for different including numbers of events centered at each calculation grid cell.

2. Data and methodology

We used the earthquake catalog maintained by the Central Weather Bureau of Taiwan. For the ETAS analysis, we chose the earthquakes with magnitudes ≧2.4 and depths shallower than 30 km. The magnitude of 2.4 corresponds to the completeness magnitude in inland Taiwan region (Mignan et al., 2011) and the depth of 30 km is roughly the thickness of the crustal seismogenic zone in this region. We excluded the grid cells with completeness magnitudes larger than 2.4 mainly in ocean region in order to focus on carefully detecting the change in seismic activity possibly caused by preseismic slip near the source area of the Chi-Chi earthquake.

The ETAS model (Ogata, 1988, 1992, 1999) was applied to systematically examine the precursory seismicity of the Chi-Chi earthquake over the whole Taiwan region. The model regards each earthquake as a realization from a point process with a conditional intensity function λ as follows:

$$\lambda(t) = \mu + \sum_{t_j<t} K \exp\left\{\alpha\left(M_j - M_c\right)\right\} \Big/ \left(t - t_j + c\right)^p. \quad (1)$$

For circular region centered at i-th grid cell, Eq. (1) can be rewritten as below:

$$\lambda_i(t) = \mu_i + \sum_{t_j<t} K_i \exp\left\{\alpha_i\left(M_j - M_c\right)\right\} \Big/ \left(t - t_j + c_i\right)^{p_i} \quad (1')$$

where λ is modeled seismic activity or modeled number of earthquakes per day, μ is occurrence rate of background seismic activity in day, which cannot be explained as the contribution of past aftershock events, M_j is magnitude of j-th earthquake, M_c is cut-off magnitude, α is a constant representing the efficiency of earthquake with a magnitude of M_j, K is a constant expressing the level of activity, c is a constant for adjusting time axis and p is a constant reflecting the temporal attenuation of seismic activity. t_j is the occurrence time of j-th

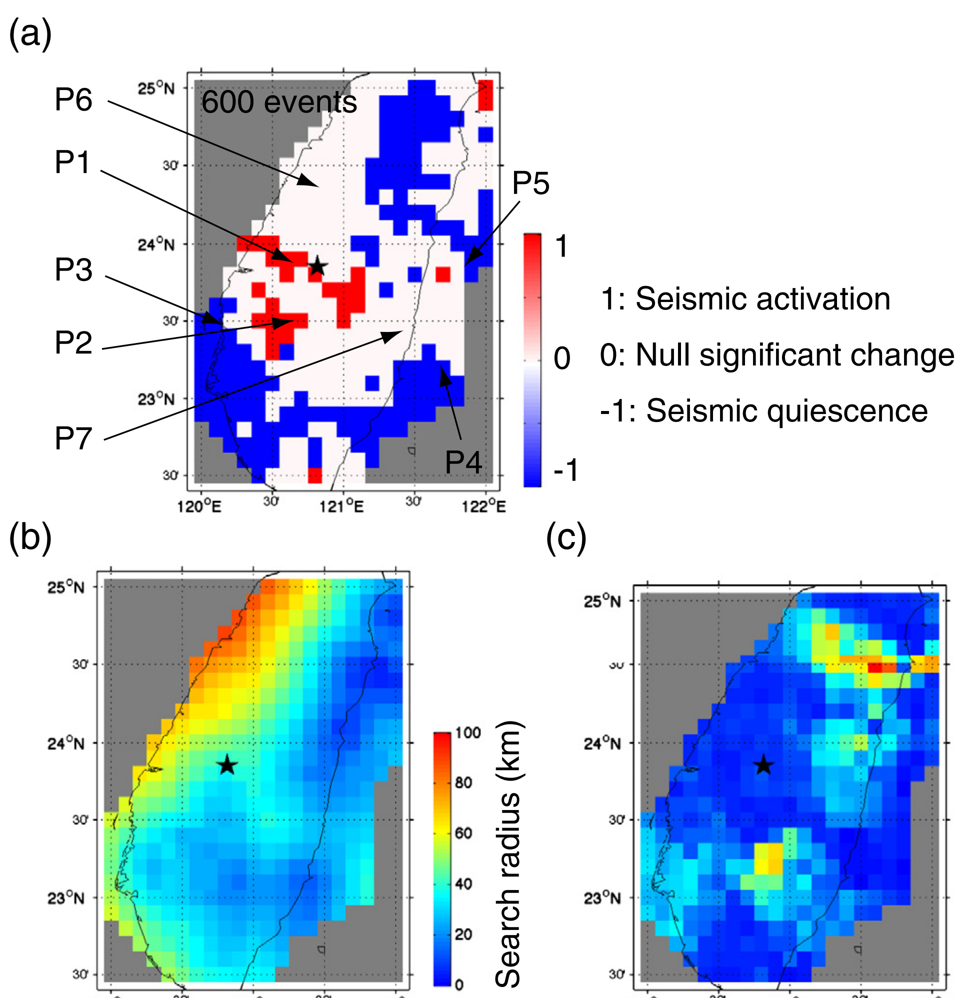

Fig. 2. (a) ETAS map: spatial distribution showing three patterns of temporal changes in seismic activities (seismic quiescence, seismic activation, and null significant change) for circular areas centered at respective calculation grid cells. Blue color mesh represents seismic quiescence for prediction period (Jan. 1, 1998–Sep. 20, 1999) relative to target period (model fitting period: Jan. 1, 1994–Dec. 31, 1997). Red color mesh denotes seismic activation. White color mesh corresponds to null significant temporal change in seismic activity. Black star represents the epicenter of the 1999 Chi-Chi earthquake. (b) Event search radius map: Spatial distribution showing the radii within which 600 events are collected for ETAS calculation. (c) Calculated value of Kormogorov–Smirnov statistics showing the goodness of model fit.

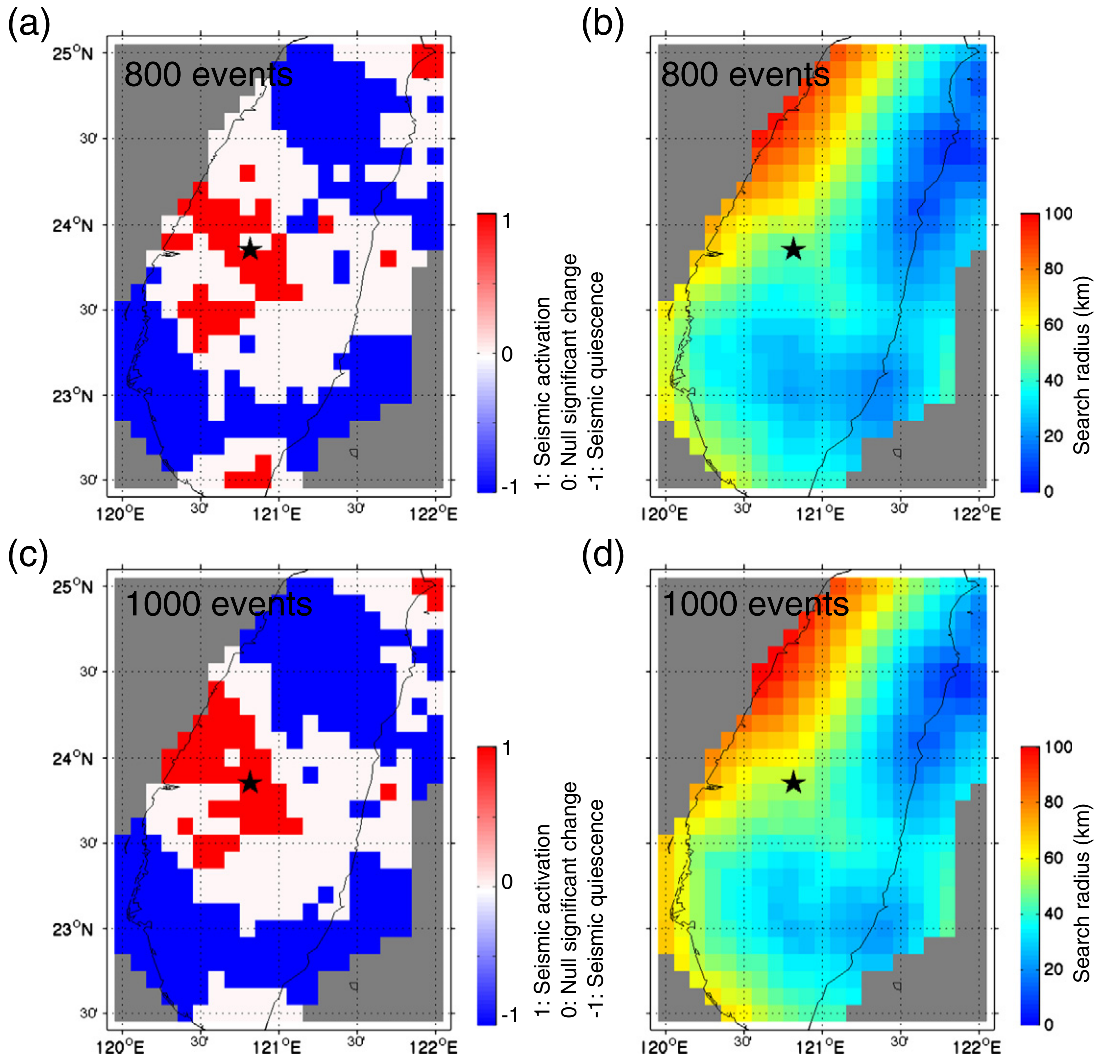

Fig. 3. ETAS maps and the corresponding event search radius maps obtained by applying the ETAS model to different including numbers of events: (a) and (b) 800 events and (c) and (d) 1000 events. Black star represents the epicenter of the Chi-Chi earthquake.

earthquake. It should be noticed that this model takes all potential aftershocks above M_c into account because it assumes that each earthquake is accompanied by its own offspring shocks, or aftershocks, whose number depends on the magnitude of parent shocks. The cumulative number of earthquakes at time t since t_s for circular region centered at i-th grid cell can be expressed as below:

$$\Lambda_i(t) = \int_{t_s}^{t}\lambda_i(s)ds = \mu_i(t-t_s) + K_i\sum_{t_j<t}\exp\left\{\alpha_i\left(M_j-M_c\right)\right\}\left\{c_i^{\,1-p_i}-\left(t-t_j+c_i\right)^{1-p_i}\right\}/(p_i-1), \tag{2}$$

where $\tau_{ij} = \Lambda_i(t_j)$ is transformed time, which is defined for i-th grid cell and is equivalent to theoretical cumulative number of earthquakes until the occurrence time t_j of j-th earthquake. Thus calculated sequence of transformed time τ_{ij} is called residual process. The advantage of using residual process is that, if there is a difference between theoretical seismic activity modeled by the ETAS model and actual activity, anomalous seismic activity such as seismic activation and quiescence that cannot be explained by the model appears in a visible manner. Because seismic quiescence (activation) can exist even in an active (quiescent) stage of seismic activity, it is not desirable to remove them beforehand.

Our ETAS analysis procedure is shown in Fig. 1. After Taiwan region is divided into grid cells with a dimension of 0.1°×0.1°(totally m grid cells), the ETAS model is applied to fit the curve of cumulative event number for circular region centered at i-th calculation grid cell $(i = 1-m)$ for a *target* period, which is discriminated from the subsequent *prediction* period in which the occurrence of anomalous seismicity change is assessed based on statistical tests a) and b) as described below and as shown in the flowchart of Fig. 1. We conducted the two statistical tests with a confidence level of 95% for carefully assessing the change in seismic activity for prediction period. Only when both statistical tests are assessed as significant and same-signed, seismic activity is regarded as seismic quiescence or seismic activation, which depends on the sign (Fig. 1). We have let the target and prediction periods from Jan. 1, 1994 to Dec. 31, 1997 and from Jan. 1, 1998 to Sep. 20, 1999 right before the Chi-Chi event, respectively. Selection of Jan. 1, 1994 as the beginning time of target period is due to the beginning of implementation of an automatic, realtime, telemetered mode of seismic network (Mignan et al., 2011; Shin et al., 1996). The statistical tests utilized are explained as following:

a) The first test assesses the significance of change in mean difference between modeled and actual cumulative earthquake numbers before and after the middle of prediction period (Fig. 1).

The purpose of this test is to investigate the existence of anomalous seismic activity especially in the latter half of prediction period rather than the first half. For example, if the deviation of actual seismic activity from theoretical one is larger in the latter half of prediction period than in the first half, the statistical test leads to the judgment that abnormal seismic activity continues up to the end of prediction period. In the modeled seismicity, the sequence of transformed times is distributed according to the stationary Poisson process (Brown et al., 2001; Papangelou, 1972). In the statistical test, prediction period is evenly divided into two transformed-time intervals and the following statistics is calculated:

$$Z_A = (R_1 - R_2) \bigg/ \sqrt{\frac{\sigma_1^2}{n_1} + \frac{\sigma_2^2}{n_2}}, \tag{3}$$

where R_1 and R_2 are the mean differences between modeled and actual cumulative earthquake numbers for the first half and the latter half transformed-time intervals, respectively; n_1 and n_2 are the numbers of earthquakes for respective transformed-time intervals; σ_1 and σ_2 are standard deviations of differences between modeled and actual cumulative earthquake numbers for respective transformed-time intervals. For i-th grid cell, Eq. (3) can be rewritten as below:

$$Z_{iA} = (R_{i1} - R_{i2}) \bigg/ \sqrt{\frac{\sigma_{i1}^2}{n_{i1}} + \frac{\sigma_{i2}^2}{n_{i2}}}. \tag{3'}$$

If Z_{iA} is significantly positive, then the change in seismic activity is regarded as seismic quiescence; If Z_{iA} is significantly negative, it is regarded as seismic activation; If Z_{iA} is not significant, it is not regarded as anomalous seismicity. Final judgment and classification of seismic activity for prediction period for each grid cell depends on the result of the following second test.

b) The second test assesses the significance of difference between the numbers of local transformed-time windows for seismic quiescence and seismic activation in prediction period (Fig. 1). The purpose of this test is to investigate the existence of seismic quiescence or seismic activation for respective local transformed-time windows in prediction period. Seismic activity for each local transformed-time window $(\tau - h, \tau)$ in prediction period is classified into three patterns: seismic quiescence, seismic activation, and null significant change; parameter h represents the width of transformed-time window; and the local transformed-time window is moved forward by a constant interval, i.e. 0.25 h. In order to classify seismic activities in respective local transformed-time windows into three patterns (seismic quiescence, seismic activation, and null significant change), we evaluated the significance of difference between the actual cumulative earthquake number and the modeled one that is calculated from the ETAS model. For example, if the number of local transformed-time windows for seismic quiescence is significantly more than that for seismic activation, the statistical test leads to the judgment that seismic quiescence is prominent in prediction period. Here, for convenience of assessing the significance of difference, the number of events ΔN in the transformed-time window $(\tau - h, \tau)$ is transformed to a variable ξ that is approximately distributed according to a normal distribution with mean 0 and variance 1 by the following equation (Ogata, 1988; Shimizu and Yuasa, 1984),

$$\xi = \xi(\Delta N, h) = \frac{33\Delta N + 29 - h - (32\Delta N + 31)[h/(\Delta N + 1)]^{1/4}}{9(\Delta N + 1)^{1/2}}. \tag{4}$$

For i-th grid cell and k-th local transformed-time window in prediction period, Eq. (4) can be rewritten as follows:

$$\xi_{ik} = \xi_{ik}(\Delta N_{ik}, h) = \frac{33\Delta N_{ik} + 29 - h - (32\Delta N_{ik} + 31)[h/(\Delta N_{ik} + 1)]^{1/4}}{9(\Delta N_{ik} + 1)^{1/2}}. \tag{4'}$$

When $\xi > 2$, seismic activation is assessed as significantly occurred in the local transformed-time window. On the contrary, when $\xi < -2$, seismic quiescence is regarded as significantly occurred. The case of $-2 \le \xi \le 2$ indicates null significant change of seismic activity in prediction period. The criteria are based on panels 3a and 3b of Fig. 15 in Ogata (1988). After counting the numbers of local transformed-time windows for seismic quiescence and seismic activation based on Eq. (4′) for i-th grid cell, the significance of difference between their counts is evaluated by the following equation:

$$Z_{iB} = \left(p_{iq} - p_{ia}\right) \bigg/ \sqrt{\left\{\left(p_{iq} + p_{ia}\right) - \left(p_{iq} - p_{ia}\right)^2\right\} \bigg/ n_{iall}}, \tag{5}$$

where p_q and p_a are the numbers of local transformed-time windows for seismic quiescence and seismic activation, respectively, which are normalized by the total number of local transformed-time windows n_{all} in prediction period. If Z_{iB} is significantly positive, then the change in seismic activity is regarded as seismic quiescence; If Z_{iB} is significantly negative, it is regarded as seismic activation; If Z_{iB} is not significant, it is not regarded as anomalous seismicity.

Based on the significances and signs of Z_{iA} and Z_{iB}, the change in seismic activity for prediction period for i-th grid cell is then classified into three patterns: seismic activation, seismic quiescence, and null significant change. If both Z_{iA} and Z_{iB} are significantly positive, then the change in seismic activity is regarded as seismic quiescence; If both Z_{iA} and Z_{iB} are significantly negative, then it is assessed as seismic activation; If at least one of Z_{iA} and Z_{iB} is insignificant or Z_{iA} and Z_{iB} have different signs, it is not regarded as anomalous seismicity. By the repetition of this calculation procedure until m-th grid cell, the ETAS map can be obtained, which shows the spatial pattern of precursory changes in seismic activities for respective grid cells (Figs. 1 and 2a).

To guarantee an appropriate fitting of the ETAS model for each grid cell, various including numbers of events were used in fitting of the ETAS model to the data (600, 800, and 1000 events in this study). We can examine the robustness of the resultant spatial pattern of temporal changes in seismic activity by using different choices of event numbers in model fittings.

3. Result

Fig. 2a shows the spatial pattern of seismicity changes in prediction period for circular area centered at every calculation grid cell and 600 including number of events, i.e. the ETAS map. This figure indicates the existence of significant seismic quiescence over broader regions outside the source area of the Chi-Chi earthquake. It should also be noticed that inland areas near the source area of the Chi-Chi earthquake showed precursory activation in seismic activity. Fig. 2b denotes the event search radius for each grid cell, within which 600 events is collected for the ETAS calculation. Smaller searching radius for a grid cell reflects higher seismic activity in its surrounding area and vice versa (Mignan et al., 2011). Fig. 2c shows the calculated value of Kormogorov–Smirnov statistics which is obtained with goodness-of-fit test (two-sample Kormogorov–Smirnov test) for the target period. This shows the goodness of model fitting to the cumulative number of events, which is classified into two categories: significant difference (poor fitting) and insignificant difference (good fitting); A value less than 6.0 corresponds to good fitting, which is

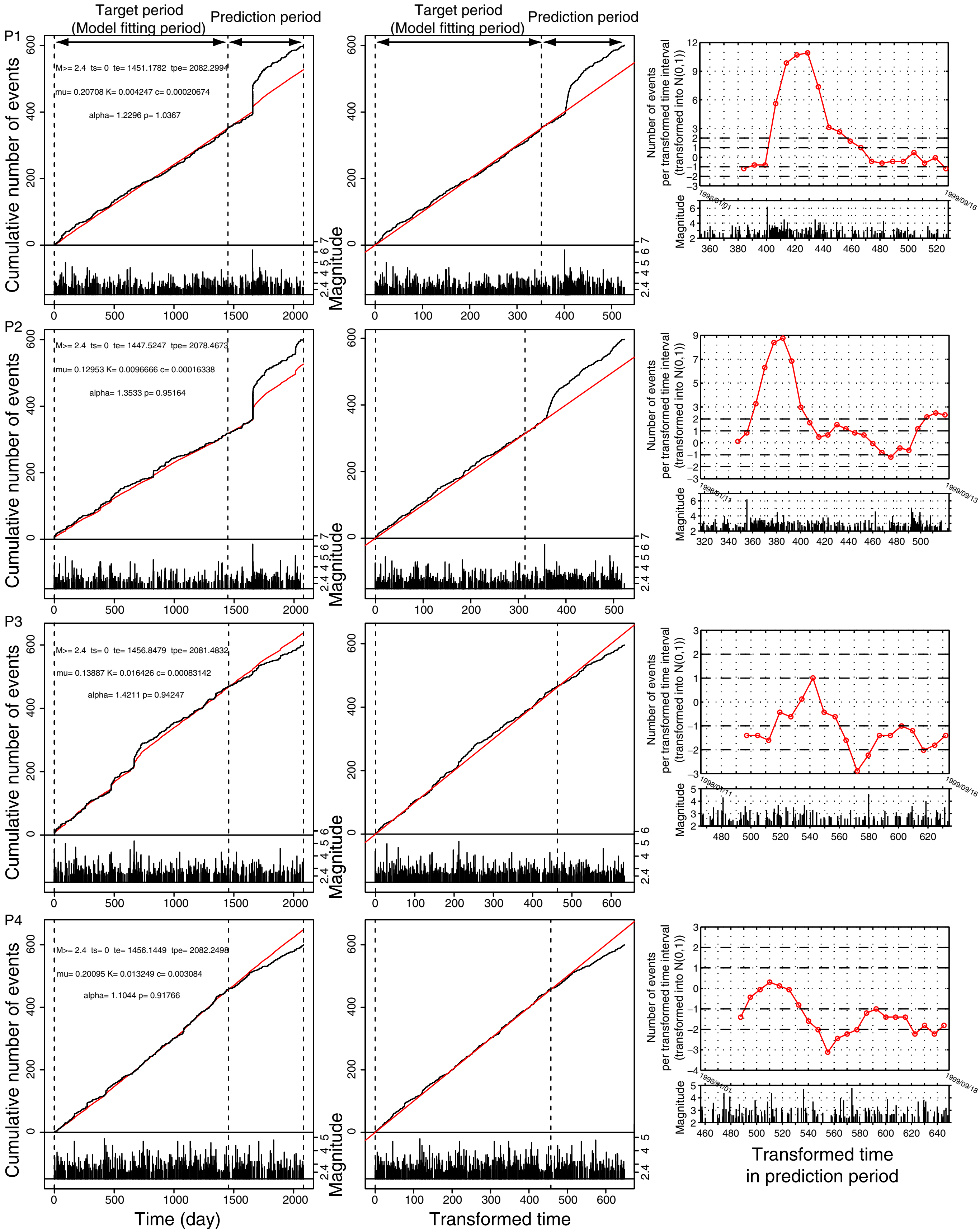

Fig. 4. First- and second-column panels show the plots of cumulative number of events against time and transformed time, respectively, for circular areas centered at calculation grid cells of P1 to P7, the locations of which are shown in Fig. 2(a). Third-column panel show the results obtained by the statistical test b) mentioned in Section 2 and Fig. 1. The vertical axis represents the number of events per unit transformed time interval, or ξ obtained by Eq. (4′) (see text in detail). The horizontal axis represents transformed time in prediction period. Dates of the first and last events in prediction period are also shown for reference.

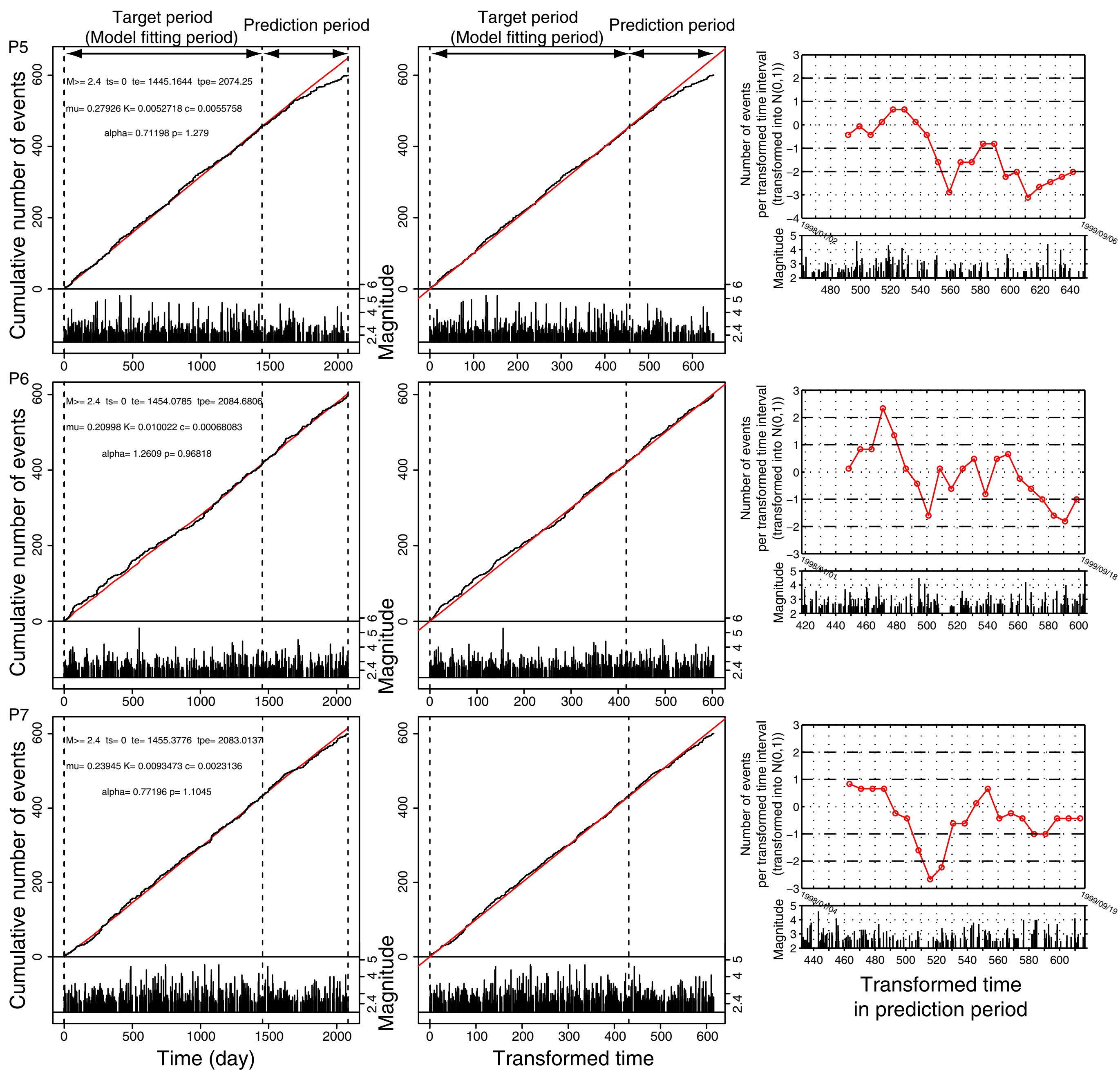

Fig. 4. (*continued*).

determined depending on the degree of freedom or the number of data sets (two data sets in this study). The occurrence of swarm-like events in target period often causes a poor fitting of the ETAS model to the data and a part of our results is no exception especially in a part of northeastern and southeastern Taiwan. This problem is discussed in Section 4 in detail.

Fig. 3 denotes the ETAS maps and their corresponding event search radius maps obtained by applying the ETAS model to different including numbers of events: (a) and (b) 800 events and (c) and (d) 1000 events. Panels (a) and (c) imply the robustness of the spatial pattern of seismic quiescence over broader regions outside the source area of the Chi-Chi earthquake and seismic activation near the source area. For both cases, apparent extensions of seismic activation and quiescence areas in northwestern Taiwan can clearly be recognized because of lower seismic activity in the region relative to that in other region, implying that including numbers of events in fitting the ETAS model to the data are too many for these cases. Seismic activation areas of the ETAS maps for including numbers of events less than 600 are almost the same and are not shown here.

The first- and second-column panels of Fig. 4 show the plots of cumulative numbers of earthquakes against time in day and transformed time, respectively, for circular area centered at each calculation grid cell of P1 to P7, the locations of which are shown in Fig. 2a. The linear trend in the second-column panel corresponds to the seismic activity distributed according to the stationary Poisson process, which is expected from the ETAS model. The first- and second-column panels of P1 and P2 show deviations in prediction period upward from the straight lines, which therefore represent the occurrences of seismic activation. On the contrary, those of P3 to P5 exhibit downward deviations from the linear trends, indicating the occurrences of seismic quiescence. In addition, the same panels of P6 and P7 show examples of null significant changes in seismic activities, which do not show any significant deviations from linear trends. Parameters t_s and t_e in the first-column panels are the beginning and end times of target interval (model fitting interval), respectively, which are denoted by the first two vertical dotted lines in the first- and second-column panels. Parameter t_{pe} shows the end time of prediction period, which corresponds to the last vertical dotted line in the first-column panels. Parameters of the ETAS models, μ, K, c, α and p, indicate the maximum likelihood estimates, which are obtained by fitting the ETAS model to the data for target interval. Third-column panels of Fig. 4 shows the results obtained by the statistical test b) as mentioned in Section 2 and shown in Fig. 1. The horizontal axis represents transformed time. Dates of the first and last events are also shown for reference. The beginning and end times for each third-column panel are different depending on the occurrence times of the beginning and last events in prediction period. The vertical axis represents the number of events per unit transformed time interval, i.e. ξ obtained by Eq. (4′). Width of transformed time window (h) for which seismic activity is assessed is 30 (1/day); Moving step of transformed time window is 0.25 h (1/day). It should be noted that the number ξ for grid cell P1 are larger than 2 for transformed time intervals of nearly 410 to 450, roughly corresponding to a time span from middle 1998 to late 1998. Because the number of windows with $\xi > 2$ is significantly more than that with $\xi < -2$, seismic activity in prediction period for the grid cell is regarded as seismic activation. The number ξ shown for grid cell P2 are also larger than 2 for transformed time intervals of nearly 360 to 400 and 520 to 590, the latter of which is due to a local effect near the grid cell. On the contrary, for grid cells P3 to P5, the number of windows with $\xi < -2$ is significantly more than that with $\xi > 2$, which represents the occurrences of seismic quiescence. For grid cell P6 and P7, there is no significant difference between the numbers of windows with $\xi > 2$ and $\xi < -2$ or there is neither windows with $\xi > 2$ nor those with $\xi < -2$. Threshold values of -2 and 2 are based on the criteria by panels 3a and 3b of Fig. 15 in Ogata (1988).

4. Discussion and conclusions

We applied the ETAS model to the earthquake catalog of Taiwan region prior to the occurrence of the 1999 Chi-Chi earthquake. Significant seismic quiescence was found over broader regions outside its source area. This result is consistent with that obtained with the ZMAP method by Wu and Chiao (2006) and Wu and Chen (2007). We also found inland areas for precursory seismic activation near the source area of the Chi-Chi earthquake, which are again consistent with the existence of anomalous seismic activities as indicated by Chen and Wu (2006).

In fitting the ETAS model to the data, as shown in Fig. 2c, goodness of fit is lower especially in northeastern Taiwan (121.6°E, 24.5°N) and in southeastern Taiwan (120.8°E, 23.2°N), which is caused by the occurrence of swarm-like events near the grid cells. In order to address the problem, it may be an approach that target period is further divided into more-than-one time intervals, and that the ETAS model is applied to the local time interval including swarm-like events to obtain another parameter estimates. This procedure is, however, considerably complicated and time-consuming. This problem is, therefore, out of consideration in this study, and is an issue to be worked on in the future.

What is the occurrence mechanism of seismic quiescence over broader regions of Taiwan? By a numerical simulation using rate- and state-dependent friction laws (Ruina, 1983), Kato et al. (1997) demonstrated the appearance of regional seismic quiescence in the continental crust before a large interplate earthquake due to the regional stress relaxation could be caused by preseismic sliding on a boundary between a subducting oceanic plate and the overriding continental plate. Kato et al. (1997) also argues that the mechanism of the seismic quiescence can also be applied to other types of earthquakes, such as intraplate earthquakes on active faults. Seismic quiescence obtained by this study and by previous studies of Wu and Chiao (2006) and Wu et al. (2008) may thus reflect the temporal change in crustal seismicity associated with the regional stress relaxation prior to the Chi-Chi earthquake. In addition, there is a previous study indicating an abnormal geodetic observation prior to the Chi-Chi earthquake. By analyzing the GPS dataset of a continuous mode station (S103) (Yu et al., 1997) close to the southern edge of surface rupture caused by the Chi-Chi earthquake, Hou et al. (2003) found the east–west shortening rate started decreasing from the spring of 1998 and turned to showing extension mode after the summer of the year. They interpreted this change as due to the stress drop immediately before the Chi-Chi earthquake. Our result indicating the existence of seismic activation for grid cells near the source area of the Chi-Chi earthquake may have been caused by precursory slip on the fault plane.

For comprehensively understanding the mechanism of preparatory process of the Chi-Chi earthquake, it is required to explain not only the seismic quiescence but also the seismic activation obtained in this study and in previous studies such as Chen et al. (2005), Chen and Wu (2006) and Wu et al. (2008). With the Pattern Informatics (PI) method, Wu et al. (2008) demonstrated that areas of anomalous seismic activities indicated by the PI hotspots migrated toward the epicenter of the Chi-Chi earthquake. That would also reflect different aspects of the precursory seismicity associated with the Chi-Chi earthquake. It is important to integrate these results of seismicity anomalies for understanding the preparatory process of the Chi-Chi earthquake and for improving our knowledge about large earthquakes. In this study, only the earthquake catalog was used to characterize the precursory change in seismic activity. It would also be important to integrate other kinds of geophysical data such as dilatation rate for comprehensively understanding the physical mechanism leading to the occurrence of a large crustal earthquake (Hsu et al., 2009). This is because respective kinds of physical data is considered to reflect different aspects of crustal activity including the occurrence of a large earthquake and they would give more information to shed light on the mechanism of precursory change in seismic activity. How to integrate different kinds of data is a challenging issue that needs to be tackled in the future.

Acknowledgment

We are obliged to the suggestions and comments provided by Dr. Chung-Han Chan and three anonymous reviewers, which were very instructive for improving the manuscript. The authors used the earthquake catalog maintained by the Taiwanese Central Weather Bureau. We are grateful to the bureau staffs for maintaining the catalog. This research was supported by the National Science Council (R.O.C.).

References

Borovik, N., Misharina, L., Treskov, A., 1971. On the Possibility of Strong Earthquakes in Pribakalia in the Future: Izv. Acad. Sci. USSR Phys. Solid Earth, English Transl., No. 1, pp. 13–16.

Bowman, D.D., King, G.C.P., 2001. Accelerating seismicity and stress accumulation before large earthquakes. Geophysical Research Letters 28, 4039–4042.

Bowman, D.D., Ouillon, G., Sammis, G., Sornette, A., Sornette, D., 1998. An observed test of the critical earthquake concept. Journal of Geophysical Research 103, 24359–24372.

Brown, E.N., Barbieri, R., Ventura, V., Kass, R.E., Frank, L.M., 2001. The time-rescaling theorem and its application to neural spike train data analysis. Neural Computation 14, 325–346.

Bufe, C.G., Varnes, D.J., 1993. Predictive modeling of the seismic cycle of the greater San Francisco Bay region. Journal of Geophysical Research 98, 9871–9883 (1993).

Bufe, C.G., Nishenko, S.P., Varnes, D.J., 1994. Seismicity trends and potential for large earthquakes in the Alaska–Aleutian region. Pure and Applied Geophysics 142, 83–99.

Chen, C.C., 2003. Accelerating seismicity of moderate-size earthquakes before the 1999 Chi-Chi, Taiwan, earthquake: testing time-prediction of the self-organizing spinodal model of earthquakes. Geophysical Journal International 155, F1–F5.

Chen, C.C., Wu, Y.X., 2006. An improved region–time–length algorithm applied to the 1999 Chi-Chi, Taiwan earthquake. Geophysical Journal International 166, 1144–1147.

Chen, C.C., Rundle, J.B., Holliday, R., Nanjo, K.Z., Turcotte, D.L., Li, S.C., Tiampo, K.F., 2005. The 1999 Chi-Chi, Taiwan, earthquake as a typical example of seismic activation and quiescence. Geophysical Research Letters 32, L22315. http://dx.doi.org/10.1029/2005GL023991.

Chen, C.C., Rundle, J.B., Li, H.C., Holliday, J.R., Nanjo, K.Z., Turcotte, D.L., Tiampo, K.F., 2006. From tornadoes to earthquakes: forecast verification for binary events applied to the 1999 Chi-Chi, Taiwan, earthquake. Terrestrial Atmospheric and Oceanic Sciences 17, 503–516.

Chen, C.-C., Telesca, L., Ma, K.-F., Lin, Y.-Y., 2010. Scaling in spectral behavior of regional to single-fault seismicity. Europhysics Letters 90, 48004.

Chen, C.-C., Telesca, L., Lee, C.-T., Sun, Y.-S., 2011. Statistical physics of landslides: new paradigm. Europhysics Letters 95, 49001.

Console, R., Montuori, C., Murru, M., 2000. Statistical assessment of seismicity patterns in Italy: are they precursors of subsequent events? Journal of Seismic 4, 435–449.

Habermann, R.E., 1988. Precursory seismic quiescence: past, present, and future. Pure and Applied Geophysics 126, 279–318.

Habermann, R.E., Wyss, M., 1984. Background seismicity rates and precursory seismic quiescence: Imperial Valley, California. Bulletin of the Seismological Society of America 74, 1743–1755.

Holliday, J.R., Nanjo, K.Z., Tiampo, K.F., Rundle, J.B., Turcotte, D.L., Donnellan, A., 2005. Forecasting the locations of future earthquake and its verification. Nonlinear Processes in Geophysics 12, 965–977.

Holliday, J.R., Rundle, J.B., Tiampo, K.F., Klein, W., Donnellan, A., 2006. Systematic procedural and sensitivity analysis of the pattern informatics method for forecasting large ($M \geq 5$) earthquake events in southern California. Pure and Applied Geophysics 12, 965–977.

Hou, C., Chen, Y., Hu, J., Lin, C., Yu, S., Chen, C., Wang, J., 2003. Feasibility study on earthquake precursor using GPS data in Taiwan. American Geophysical Union, Fall Meeting 2003, abstract #T12C-0478.

Hsu, Y.J., Yu, S.B., Simons, M., Kuo, L.C., Chen, H.Y., 2009. Interseismic crustal deformation in the Taiwan plate boundary zone revealed by GPS observations, seismicity, and earthquake focal mechanisms. Tectonophysics 479, 4–18.

Jaume, S.C., Sykes, L.R., 1999. Evolving towards a circular point: a review of accelerating seismic moment/energy release prior to large and great earthquakes. Pure and Applied Geophysics 155, 279–306.

Karakaisis, G.F., Papazachos, C.B., Savvaidis, A.S., Papazachos, B.C., 2002. Accelerating seismic crustal deformation in the North Aegean Trough, Greece. Geophysical Journal International 148, 193–200.

Kato, N., Ohtake, M., Hirasawa, T., 1997. Possible mechanism of precursory seismic quiescence: regional stress relaxation due to preseismic sliding. Pure and Applied Geophysics 150, 249–267.

Mignan, A., 2011. Retrospective on the accelerating seismic release (ASR) hypothesis: controversy and new horizons. Tectonophysics 505, 1–16.

Mignan, A., Werner, M.J., Wiemer, S., Chen, C.-C., 2011. Bayesian estimation of the spatially varying completeness magnitude of earthquake catalogs. Bulletin of the Seismological Society of America 101, 1371–1385.

Mogi, K., 1969. Some features of recent seismic activity in and near Japan (2). Bulletin of the Earthquake Research Institute 46, 30–36.

Ogata, Y., 1988. Statistical models for eathquake occurrences and residual analysis for point processes. Journal of the American Statistical Association 83 (401), 9–27.

Ogata, Y., 1992. Detection of precursory relative quiescence before great earthquakes through a statistical model. Journal of Geophysical Research 97, 19845–19871.

Ogata, Y., 1999. Seismicity analysis through point-process modeling: a review. Pure and Applied Geophysics 155, 471–507.

Papangelou, F., 1972. Integrability of expected increments of point processes and a related random change of scale. Transactions of the American Mathematical Society 165, 483–506.

Papazachos, B.C., Karakaisis, G.F., Scordilis, E.M., Papazachos, C.B., Panagiotopoulos, D.G., 2010. Present patterns of decelerating–accelerating seismic strain in South Japan. Journal of Seismology 14. http://dx.doi.org/10.1007/s10950-009-9165-z.

Resenberg, P.A., Matthews, M.V., 1988. Precursory seismic quiescence: a preliminary assessment of the hypothesis. Pure and Applied Geophysics 126, 373–406.

Ruina, A.L., 1983. Slip instability and state variable friction laws. Journal of Geophysical Research 88, 10359–10370.

Rundle, J.B., Turcotte, D.L., Shcherbakov, R., Klein, W., Sammis, C., 2003. Statistical physics approach to understanding the multiscale dynamics of earthquake fault systems. Reviews of Geophysics 41 (4), 1019. http://dx.doi.org/10.1029/2003RG000135.

Shimizu, R., Yuasa, M., 1984. Normal approximation for asymmetric distributions. Proceedings of the Institute of Statistical Mathematics 32, 141–158.

Shin, T.C., Tsai, Y.B., Wu, Y.M., 1996. Rapid response of large earthquakes in Taiwan using a realtime telemetered network of digital accelerographs. Proc. 11th World Conf. Earthq. Eng., Paper No. 2137.

Sornette, D., Sammis, C.G., 1995. Complex critical exponents from re-normalization group theory of earthquakes: Implications for earthquake predictions. Journal de Physique I France 5, 607–619.

Sykes, L.R., Jaume, S.C., 1990. Seismic activity on neighboring faults as a long-term precursor to large earthquakes in the San Francisco Bay area. Nature 348, 595–599.

Tiampo, K.F., Rundle, J.B., McGinnis, S., Gross, S.J., Klein, W., 2002a. Eigenpatterns in southern California seismicity. Journal of Geophysical Research 107 (B12), 2354. http://dx.doi.org/10.1029/2001JB000562.

Tiampo, K.F., Rundle, J.B., McGinnis, S., Gross, S.J., Klein, W., 2002b. Mean-field threshold systems and phase dynamics: an application to earthquake fault systems. Europhysics Letters 60, 481–487.

Wei, G., Lin, Z., Zhu, X., Zhao, Y., Zhao, X., Hou, H., 1978. On seismic gaps previous to certain great earthquakes occurred in north China. Acta Geophysica Sinica 21, 213–217.

Wiemer, S., Wyss, M., 1994. Seismic quiescence before the Landers ($M = 7.5$) and Big Bear ($M = 6.5$) 1992 earthquakes. Bulletin of the Seismological Society of America 84, 900–916.

Wu, Y.M., Chen, C.C., 2007. Seismic reversal pattern for the 1999 Chi-Chi, Taiwan, Mw7.6 earthquake. Tectonophysics 429, 125–132.

Wu, Y.M., Chiao, L.Y., 2006. Seismic quiescence before the 1999 Chi-Chi, Taiwan, Mw7.6 earthquake. Bulletin of the Seismological Society of America 96, 321–327.

Wu, Y.H., Chen, C.C., Rundle, J.B., 2008. Detecting precursory earthquake migration patterns using the pattern informatics method. Geophysical Research Letters 35, L19304. http://dx.doi.org/10.1029/2008GL035215.

Wyss, M., Wiemer, S., 1997. Two current seismic quiescences within 40 km of Tokyo. Geophysical Journal International 128, 459–473.

Yu, S.B., Chen, H.Y., Kuo, L.C., 1997. Velocity field of GPS stations in the Taiwan area. Tectonophysics 274, 41–59.